Eur. Phys. J. D **26**, 275–283 (2003)
DOI: 10.1140/epjd/e2003-00258-6

THE EUROPEAN PHYSICAL JOURNAL D

Analysis of the merger between plasma vortices in a Penning trap

G.G.M. Coppa[a], A. D'Angola[b], F. Peano, and F. Peinetti

Istituto Nazionale per la Fisica della Materia (INFM) and Dipartimento di Energetica, Politecnico di Torino, corso Duca degli Abruzzi 24, 10129 Torino, Italy

Received 18 April 2003
Published online 12 August 2003 –

Abstract. In the paper, the interaction between a finite-size vortex of constant density and a weak, pointlike vortex in a Penning trap is studied analytically. A suitable Fourier representation for the contour of the finite vortex is considered and a model for small perturbations, which is linear with respect to the Fourier coefficients, is deduced. The resonance condition for the surface modes and a sufficient condition for the merger of the vortices not to occur are obtained. The validity of the analytic results is checked with a contour dynamics code making use of a new methodology developed by the authors. Numerical results referred to a case of strongly-interacting vortices are also reported.

PACS. 52.27.Jt Nonneutral plasmas – 52.35.We Plasma vorticity – 47.32.Cc Vortex dynamics

1 Introduction

An important issue in two-dimensional inviscid fluid dynamics is the study of the merger of vortices. The merging process between two vortices of comparable size and vorticity has been extensively studied, both experimentally and numerically [1–5]. Moreover, an analytical model has been proposed by O'Neil *et al.* [6] to study the merger in an infinite domain, when one of the two vortices can be regarded as a weak, pointlike vortex. In this paper, the approach is generalized to systems with cylindrical boundary: due to the analogy between incompressible, inviscid fluids and nonneutral plasmas [7], the analysis can be used to study the merger of two plasma vortices confined in a Malmberg-Penning trap [8]. The theory presented in the paper describes the interaction of a point vortex with the surface waves of an extended vortex having constant density. When the charge of the two vortices is comparable, the evolution of such a system is strongly non linear: numerical simulations for a typical example are presented in Figures 1 and 2, showing the evolution at different times for a vortex configuration studied by Fajans *et al.* [8]. As shown in Figure 1, the evolution of two vortices is characterized by an intensive filamentation of the extended vortex, during its wrapping around the point vortex: filaments become longer and, consequently, thinner, giving rise to the Kelvin-Helmoltz instability. Details showing the wrapping process and the incoming instability are reported in Figure 2. The charge distributions have been obtained by means of a contour dynamics (CD) code developed by some of the authors [9]. The new methodology employed in the code allows one to attain a high level of accuracy: for this reason, all the results obtained with the CD code presented in Figures 1, 2 and in the paper can be regarded as reference for the problems considered.

An analytical study of the vortex interaction can be performed if the charge of the point vortex is small when compared to the total charge of the finite one. In fact, starting from the equations governing the evolution of the contour of the finite vortex, suitable approximations can be introduced by supposing the amplitude of the surface waves to be small with respect to the size of the vortex itself. Hence, an analytical theory has been developed for the case of weakly-interacting vortices and its validity has been checked by using the contour dynamics code. In the paper, the following issues are discussed:

- the description of the model for the evolution of the contour of a finite vortex (Sect. 2);
- the deduction of an analytic expression for the constants of motion predicted by the model (Sect. 3);
- the study of resonant configurations and of the trapped orbits for the point vortex; the analysis provides a sufficient condition for the vortex merger not to occur (Sect. 4);

[a] e-mail: gianni.coppa@polito.it
[b] *Present address*: Università della Basilicata, Dipartimento di Ingegneria e Fisica dell'ambiente, Contrada Macchia Romana, 85100 Potenza, Italy.

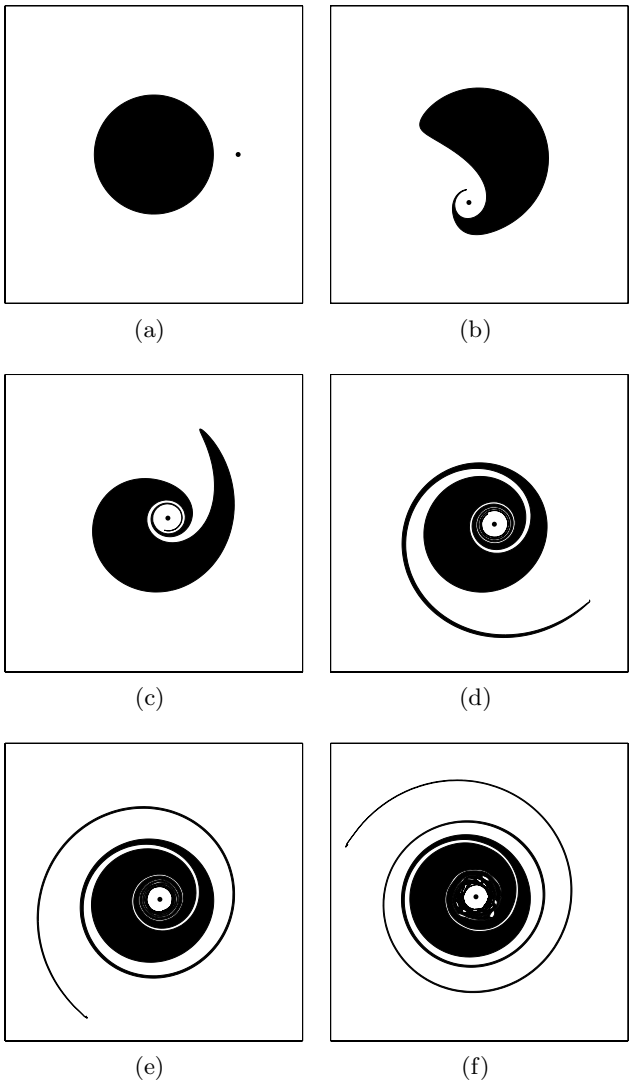

Fig. 1. Evolution of the merging process between two strongly interacting vortices: initial plasma distribution (a) and distributions after 0.5 (b), 1 (c), 2 (d), 3 (e) and 4 (f) rotations of the extended vortex.

– further considerations on a merger process and comparisons with results obtained by means of the contour dynamics technique (Sect. 5).

2 Definition of the model

In the work, the study is carried out in the framework of the dynamics of a non-neutral electron plasma. In the following, a plasma configuration made of an extended vortex and of a point vortex is considered. It must be noticed that a small, finite-sized vortex can be approximated by means of a point vortex as far as it is intense enough to avoid its shearing apart in the velocity field of the extended vortex (a quantitative analysis is reported in Ref. [6]). The extended vortex is circular (of radius r_0) and is placed initially in the center of a Penning trap (having radius R);

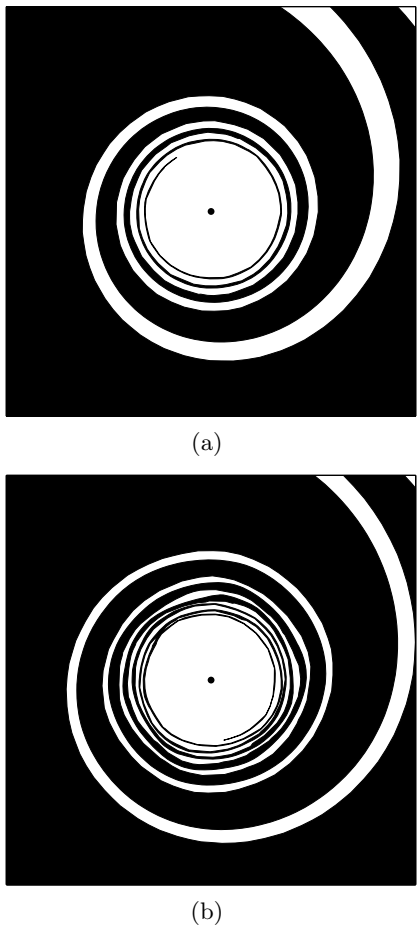

Fig. 2. Evolution of the merging process between two strongly interacting vortices: enlargements of the regions marked by a dotted line in Figure 1d (a) and in Figure 1e (b).

the particle density within the vortex has a constant value, n_0. The charge per unit length of the point vortex, $-q$, is assumed to be small with respect to the total charge per unit length of the finite vortex, $-Q$, with $Q = \pi e n_0 r_0^2$, so that the parameter $\gamma = q/Q$ is regarded to be $\ll 1$.

In order to study the evolution of the contour of the finite-size vortex, the quantity $r_c(\theta, t)$ is introduced, defined as the radial coordinate of the contour of the vortex in the angular direction θ, at time t. A point P of coordinates $(r_c(\theta(t), t), \theta(t))$ on the contour of the vortex evolves in time according to the $\mathbf{E} \times \mathbf{B}$ drift:

$$\frac{\mathrm{d}P}{\mathrm{d}t} = v_r \widehat{\mathbf{e}}_r + v_\theta \widehat{\mathbf{e}}_\theta = \frac{1}{B_0} \mathbf{E} \times \widehat{\mathbf{e}}_z. \tag{1}$$

By taking the total time derivative of P and considering its radial component, one obtains

$$v_r = \frac{\partial r_c}{\partial t} + \frac{\partial r_c}{\partial \theta} \frac{\mathrm{d}\theta}{\mathrm{d}t} \tag{2}$$

or, equivalently,

$$\frac{\partial r_c}{\partial t} = v_r - \omega \frac{\partial r_c}{\partial \theta} \tag{3}$$

being $\omega = v_\theta(r_c, \theta)/r_c$. By setting $\varepsilon(\theta, t) = r_c(\theta, t) - r_0$, and assuming $|\varepsilon| \ll r_0$, equation (3) can be expanded at first order with respect to $\varepsilon(\theta, t)$. Moreover, by expressing $\varepsilon(\theta, t)$ by means of a Fourier expansion

$$\varepsilon(\theta, t) = \sum_{m=-\infty}^{+\infty} C_m(t) \mathrm{e}^{\mathrm{i}m\theta} \tag{4}$$

from equation (3) a set of linear equations for the coefficients $\{C_m(t)\}$ is deduced. To obtain a closed set of equations for the evolution of the two-vortex distribution, the equations of motion for the point vortex, of coordinates (r_v, θ_v), must be included in the model:

$$\begin{cases} \dfrac{\mathrm{d}r_v}{\mathrm{d}t} = -\dfrac{E_{v,\theta}}{B_0} \\ \dfrac{\mathrm{d}\theta_v}{\mathrm{d}t} = \dfrac{E_{v,r}}{r_v B_0} \end{cases} \tag{5}$$

where $\mathbf{E}_v = E_{v,r}\widehat{\mathbf{e}}_r + E_{v,\theta}\widehat{\mathbf{e}}_\theta$ is the electric field acting on the point vortex. The electrostatic potential generated by the whole distribution, $\Phi(\mathbf{r}, t)$, can be written as the sum of the potential due to the finite vortex, $\phi(\mathbf{r}, t)$, and the potential due to the point vortex, $\varphi(\mathbf{r}, t)$. The potential ϕ can be determined by solving the Poisson

$$\begin{cases} \nabla^2\phi = \dfrac{en}{\varepsilon_0} \\ \phi(R, \theta) = 0 \end{cases} \tag{6}$$

where $n(\mathbf{r}, t)$ is the particle density of the finite-size vortex:

$$n(\mathbf{r}, t) = \begin{cases} n_0 & r < r_c(\theta, t) \\ 0 & r > r_c(\theta, t) \end{cases}. \tag{7}$$

Consequently, the potential ϕ can be expressed as follows:

$$\phi(\mathbf{r}, t) = \frac{en_0}{\varepsilon_0} \int_0^{2\pi} \int_0^{r_c(\theta', t)} G(r' \to r, \theta' - \theta) r' \mathrm{d}r' \mathrm{d}\theta' \tag{8}$$

where

$$G(r' \to r, \theta' - \theta) = \frac{1}{2\pi} \left[\log|\mathbf{r}' - \mathbf{r}| - \log\left| \frac{R}{r'}\mathbf{r}' - \frac{r'}{R}\mathbf{r} \right| \right] \tag{9}$$

is the Green function for the Poisson equation, *i.e.* the solution of the problem

$$\begin{cases} \nabla^2 G(r' \to r, \theta' - \theta) = \dfrac{1}{r'} \delta(r - r') \, \delta(\theta - \theta') \\ G(r' \to R, \theta' - \theta) = 0 \end{cases}. \tag{10}$$

Being $|\varepsilon(\theta, t)| / r_0 \ll 1$, a first-order expansion of ϕ with respect to ε can be considered and the following expression for ϕ is readily obtained:

$$\begin{aligned} \phi(\mathbf{r}, t) \simeq \frac{en_0}{\varepsilon_0} \int_0^{2\pi} \int_0^{r_0} G(r' \to r, \theta' - \theta) r' \mathrm{d}r' \mathrm{d}\theta' \\ + \frac{en_0}{\varepsilon_0} r_0 \int_0^{2\pi} G(r_0 \to r, \theta' - \theta) \varepsilon(\theta', t) \mathrm{d}\theta'. \end{aligned} \tag{11}$$

The same expression for ϕ would be obtained by considering a density distribution of the form:

$$n(\mathbf{r}, t) = n^{(0)}(r) + n_0 \varepsilon(\theta, t) \delta(r - r_0) \tag{12}$$

being $n^{(0)}(r)$ the density field of the unperturbed vortex.

By inserting the expansion (4) into equation (11), the second integral can be rewritten as

$$\begin{aligned} \int_0^{2\pi} G(r_0 \to r, \theta' - \theta) \varepsilon(\theta', t) \mathrm{d}\theta' = \\ \sum_{m=-\infty}^{+\infty} C_m \mathrm{e}^{\mathrm{i}m\theta} \int_0^{2\pi} G(r_0 \to r, \theta'') \mathrm{e}^{-\mathrm{i}m\theta''} \mathrm{d}\theta''. \end{aligned} \tag{13}$$

Consequently, a Fourier expansion can be considered for the potential ϕ, as

$$\phi(\mathbf{r}, t) = \phi^{(0)}(r) + \sum_{m=-\infty}^{+\infty} \phi_m(r, t) \mathrm{e}^{\mathrm{i}m\theta} \tag{14}$$

being $\phi^{(0)}(r)$ the potential created by the unperturbed vortex,

$$\phi^{(0)}(r) = \begin{cases} \dfrac{en_0}{4\varepsilon_0} \left[r^2 + r_0^2 \left(2 \log\left(\dfrac{r_0}{R} - 1 \right) \right) \right] & r < r_0 \\ \dfrac{en_0}{2\varepsilon_0} r_0^2 \log\left(\dfrac{r}{R} \right) & r > r_0 \end{cases} \tag{15}$$

and with

$$\phi_m(r, t) = \frac{2\pi en_0}{\varepsilon_0} r_0 G_m(r_0 \to r) \, C_m \tag{16}$$

where $\{G_m(r' \to r)\}$ are the Fourier components of the Green function,

$$G_m(r' \to r) = \frac{1}{2\pi} \int_0^{2\pi} G(r' \to r, \theta'') \mathrm{e}^{-\mathrm{i}m\theta''} \mathrm{d}\theta''. \tag{17}$$

The contribution to the electrostatic potential due to the point vortex, $\varphi(r, \theta)$, is evaluated immediately in terms of the Green function (10):

$$\begin{aligned} \varphi(r, \theta) &= \frac{q}{\varepsilon_0} G(r_v \to r, \theta_v - \theta) \\ &= \frac{q}{\varepsilon_0} \sum_{m=-\infty}^{+\infty} G_m(r_v \to r) \mathrm{e}^{\mathrm{i}m(\theta - \theta_v)}. \end{aligned} \tag{18}$$

From equations (14, 16, 18), the electrostatic potential generated by the two vortices can be expressed as a function of $\{\{C_m\}, r_v, \theta_v\}$. By inserting equations (14, 18) into equation (3), the following set of equations for the coefficients $\{C_m\}$ is obtained

$$\begin{aligned} \frac{\mathrm{d}C_m}{\mathrm{d}t} = -\frac{\mathrm{i}}{r_0 B_0} m \left(\Phi_m(r_0, t) + C_m \frac{\mathrm{d}\phi^{(0)}}{\mathrm{d}r}(r_0) \right) \\ - \frac{\mathrm{i}}{r_0 B_0} \sum_{k=-\infty}^{+\infty} (m - k) \, C_{m-k}(t) \frac{\partial \Phi_k}{\partial r}(r_0, t) \end{aligned} \tag{19}$$

being

$$\Phi_m(r,t) = \phi_m(r,t) + \frac{q}{\varepsilon_0} G_m(r_v \to r) \mathrm{e}^{-\mathrm{i}m\theta_v}. \quad (20)$$

In the rest of the paper, normalized quantities are employed, in which the radius of the trap, R, the inverse of the diocotron period, τ_D ($\tau_D = 2\varepsilon_0 B_0/en_0$) and the potential $\varphi^* = en_0R^2/(2\varepsilon_0)$ are chosen as reference for length, time and potential, respectively. By introducing the following dimensionless quantities

$$\begin{aligned} &\widehat{r} = r/R, \qquad \widehat{\varepsilon} = \varepsilon/R \\ &\widehat{C}_m = C_m/R, \quad \widehat{t} = t/\tau_D \\ &\widehat{G}_m(\widehat{r}' \to \widehat{r}) = 4\pi\widehat{r}_0 G_m(r' \to r) \end{aligned} \quad (21)$$

the set of equations of motion for $\left\{\widehat{C}_m\right\}$, $\widehat{r}_v$, θ_v can be written as:

$$\begin{cases} \dfrac{\mathrm{d}\widehat{C}_m}{\mathrm{d}\widehat{t}} = -\mathrm{i}m\left[\left(1 + \dfrac{\widehat{G}_m(\widehat{r}_0 \to \widehat{r}_0)}{\widehat{r}_0}\right)\widehat{C}_m \right. \\ \qquad\qquad \left. + \dfrac{\gamma}{2}\widehat{G}_m(\widehat{r}_v \to \widehat{r}_0)\mathrm{e}^{-\mathrm{i}m\theta_v}\right] \\ \dfrac{\mathrm{d}\widehat{r}_v}{\mathrm{d}\widehat{t}} = -\dfrac{1}{\widehat{r}_v}\displaystyle\sum_{m=-\infty}^{+\infty} \mathrm{i}m\widehat{G}_m(\widehat{r}_0 \to \widehat{r}_v)\widehat{C}_m\mathrm{e}^{\mathrm{i}m\theta_v} \\ \dfrac{\mathrm{d}\theta_v}{\mathrm{d}\widehat{t}} = \dfrac{\widehat{r}_0^2}{\widehat{r}_v^2} + \dfrac{1}{\widehat{r}_v}\displaystyle\sum_{m=-\infty}^{+\infty} \dfrac{\partial\widehat{G}_m(\widehat{r}_0 \to \widehat{r}_v)}{\partial\widehat{r}_v}\widehat{C}_m\mathrm{e}^{\mathrm{i}m\theta_v} \\ \qquad\qquad + \gamma\dfrac{\widehat{r}_0^2}{1-\widehat{r}_v^2} \end{cases} \quad (22)$$

The terms proportional to $\widehat{C}_i\widehat{C}_j$ or to $\gamma\widehat{C}_i$ have been neglected, as only small perturbations are considered for $\gamma \ll 1$. The first equation (22) shows that $\mathrm{d}\widehat{C}_0/\mathrm{d}\widehat{t} = 0$: therefore, in the framework of a first-order analysis, $\widehat{C}_0$ must vanish (as $\widehat{C}_0(0) = 0$).

The analytic expression for the coefficients $\widehat{G}_m$ can be obtained by solving the problem

$$\begin{cases} \dfrac{1}{\widehat{r}}\dfrac{\mathrm{d}}{\mathrm{d}\widehat{r}}\left(\widehat{r}\dfrac{\mathrm{d}\widehat{G}_m}{\mathrm{d}\widehat{r}}\right) - \dfrac{m^2}{\widehat{r}^2}\widehat{G}_m = \dfrac{2\widehat{r}_0}{\widehat{r}'}\delta(\widehat{r} - \widehat{r}') \\ \widehat{G}_m(\widehat{r}' \to 1) = 0 \end{cases} \quad (23)$$

thus obtaining

$$\widehat{G}_m(\widehat{r}' \to \widehat{r}) = \begin{cases} -\widehat{r}_0\widehat{r}^{|m|}\left[\dfrac{\widehat{r}'^{-m} - \widehat{r}'^{m}}{m}\right], & \widehat{r} < \widehat{r}' \\ -\widehat{r}_0\widehat{r}'^{|m|}\left[\dfrac{\widehat{r}^{-m} - \widehat{r}^{m}}{m}\right], & \widehat{r} > \widehat{r}' \end{cases} \quad (24)$$

for $m \neq 0$ and

$$\widehat{G}_0(\widehat{r}' \to \widehat{r}) = \begin{cases} -2\widehat{r}_0\log(\widehat{r}'), & \widehat{r} < \widehat{r}' \\ -2\widehat{r}_0\log(\widehat{r}), & \widehat{r} > \widehat{r}' \end{cases} \quad (25)$$

for $m = 0$.

3 Constants of motion

According to the exact drift-Poisson model, the total charge, the mean square radius and the electrostatic energy are constants of motion. In the framework of the present simplified model, these quantities are expected to be constant at first order with respect to ε. In fact, a first-order evaluation of the charge (per unit length) of the finite vortex gives

$$\begin{aligned} Q(t) &= en_0 \int_0^{2\pi}\mathrm{d}\theta \int_0^{r_0+\varepsilon(\theta)} r\mathrm{d}r + O\left(\varepsilon^2\right) \\ &= \pi en_0 r_0^2 + en_0 r_0 \int_0^{2\pi}\varepsilon\mathrm{d}\theta + O\left(\varepsilon^2\right). \end{aligned} \quad (26)$$

The last integral vanishes, as it is proportional to C_0; consequently, Q is constant.

The normalized mean square radius of the distribution, σ_r^2, defined as

$$\sigma_r^2 = \frac{1}{1+\gamma}\left\langle\widehat{r}^2\right\rangle + \frac{\gamma}{1+\gamma}\widehat{r}_v^2 \quad (27)$$

being $\left\langle\widehat{r}^2\right\rangle$ the normalized mean square radius of the finite size vortex, can be written (at first order with respect to $\varepsilon(\theta,t)$) as

$$\begin{aligned} \left\langle\widehat{r}^2\right\rangle &= \frac{1}{\pi\widehat{r}_0^2}\int_0^{2\pi}\mathrm{d}\theta \int_0^{\widehat{r}_0+\widehat{\varepsilon}(\theta)} \widehat{r}^3\mathrm{d}\widehat{r} + O\left(\varepsilon^2\right) \\ &= \frac{\widehat{r}_0^2}{2} + \frac{\widehat{r}_0}{\pi}\int_0^{2\pi}\widehat{\varepsilon}\mathrm{d}\theta + O\left(\varepsilon^2\right) = \frac{\widehat{r}_0^2}{2} + O\left(\varepsilon^2\right). \end{aligned} \quad (28)$$

This means that σ_r^2 is a first-order constant if $\widehat{r}_v^2$ is constant (at first order). In fact, by means of the second equation (22) and making use of expressions (25) for $\widehat{G}_m$, one can write

$$\begin{aligned} \frac{\mathrm{d}\widehat{r}_v^2}{\mathrm{d}t} = 2\widehat{r}_v\frac{\mathrm{d}\widehat{r}_v}{\mathrm{d}t} = 4\pi\mathrm{i}\sum_{m=1}^{+\infty}\widehat{r}_0^{m+1}\left[\widehat{r}_v^m - \widehat{r}_v^{-m}\right] \\ \times\left(\widehat{C}_m\mathrm{e}^{\mathrm{i}m\theta_v} - \widehat{C}_{-m}\mathrm{e}^{-\mathrm{i}m\theta_v}\right) \end{aligned} \quad (29)$$

while, using the first equation (22), the time derivative of the quantity $|\widehat{C}_m|^2$ can be evaluated as

$$\begin{aligned} \frac{\mathrm{d}}{\mathrm{d}t}\left|\widehat{C}_m\right|^2 = \gamma\pi\mathrm{i}\widehat{r}_0^{m+1}\left[\widehat{r}_v^m - \widehat{r}_v^{-m}\right] \\ \times\left(\widehat{C}_m\mathrm{e}^{\mathrm{i}m\theta_v} - \widehat{C}_{-m}\mathrm{e}^{-\mathrm{i}m\theta_v}\right). \end{aligned}$$

Therefore, the following relation between $\widehat{r}_v$ and the set of coefficients $\{\widehat{C}_m\}$ holds:

$$\frac{\mathrm{d}\widehat{r}_v^2}{\mathrm{d}t} = -\frac{4}{\gamma}\sum_{m=1}^{+\infty}\frac{\mathrm{d}}{\mathrm{d}t}\left|\widehat{C}_m\right|^2. \quad (30)$$

Equation (30) proves that σ_r^2 is a first-order constant; in addition, it shows that the quantity

$$\widehat{L} = \gamma \widehat{r}_v^2 + 4 \sum_{m=1}^{+\infty} \left| \widehat{C}_m \right|^2 \tag{31}$$

is an exact constant of motion for the present model.

As the expression for the electrostatic energy in presence of both point and continuous charge distributions is not completely obvious, the calculation is reported in some details. When a single point vortex of charge q is present, it is subject only to the electric field due to the image charge; the energy, $\mathcal{E}_p$, can be evaluated as the work done by the electrostatic forces of the image-charge field when the vortex moves from the center of the trap to the radial position r:

$$\mathcal{E}_p = -\int_0^r \frac{q^2}{2\pi\varepsilon_0} \frac{r'}{R^2 - r'^2} \mathrm{d}r' = \frac{q^2}{4\pi\varepsilon_0} \log\left(1 - \widehat{r}^2\right) \tag{32}$$

or, equivalently, as

$$\mathcal{E}_p = \frac{1}{2} q \widetilde{\varphi}\left(r\right) \tag{33}$$

being $\widetilde{\varphi}\left(r\right)$ the potential due to the image charge. When N point vortices are present, the electrostatic energy can be written as the sum of the energy of each vortex and of the interaction energy between couples of vortices:

$$\mathcal{E}_N = \frac{1}{2} \sum_{i,j \neq i} q_i \varphi_j\left(\mathbf{r}_i\right) + \sum_i \mathcal{E}_{p,i}. \tag{34}$$

By considering the limit for a continuous distribution of charge, the second term in equation (34) vanishes and one obtains the well-known expression

$$\mathcal{E} = \frac{1}{2} \int_0^{2\pi} \int_0^{r_0 + \varepsilon(\theta)} \rho(\mathbf{r}, t) \Phi(\mathbf{r}) r \mathrm{d}r \mathrm{d}\theta \tag{35}$$

where ρ is the charge density. Thus, for the physical system considered in the present work, the electrostatic energy, $\mathcal{E}$, can be written as

$$\mathcal{E} = -\frac{1}{2} \int_0^{2\pi} \int_0^{r_0 + \varepsilon(\theta)} e n(\mathbf{r}, t) \Phi(\mathbf{r}) r \mathrm{d}r \mathrm{d}\theta - \frac{1}{2} q \phi(\mathbf{r}_v) + \frac{q^2}{4\pi\varepsilon_0} \log\left(1 - \widehat{r}_v^2\right). \tag{36}$$

By taking the first-order approximations for ϕ and n with respect to ε (Eq. (12)) and defining a dimensionless energy, $\widehat{\mathcal{E}}$, as

$$\widehat{\mathcal{E}} = \frac{\mathcal{E}}{\varphi^* Q/2} \tag{37}$$

one obtains

$$\widehat{\mathcal{E}} = 2\gamma \widehat{r}_0 \sum_{m=1}^{+\infty} \widehat{r}_0^m \left[\frac{\widehat{r}_v^{-m} - \widehat{r}_v^m}{m} \right] \left(\widehat{C}_m \mathrm{e}^{\mathrm{i}m\theta_v} + \widehat{C}_{-m} \mathrm{e}^{-\mathrm{i}m\theta_v} \right) - 2\gamma \widehat{r}_0^2 \log\left(\widehat{r}_v\right) + \gamma^2 \widehat{r}_0^2 \log\left(1 - \widehat{r}_v^2\right) + 4 \sum_{m=1}^{+\infty} \left| \widehat{C}_m \right|^2 \left[\frac{1 - \widehat{r}_0^{2m}}{m} \right]. \tag{38}$$

From the equations of motion (22), the time derivative of $\widehat{\mathcal{E}}$ can be evaluated as

$$\frac{\mathrm{d}\widehat{\mathcal{E}}}{\mathrm{d}t} = 4 \sum_{m=1}^{+\infty} \frac{\mathrm{d}}{\mathrm{d}t} \left| \widehat{C}_m \right|^2 \tag{39}$$

and therefore $\widehat{\mathcal{E}}$ is a first-order constant. In addition, a second exact constant of motion for the present model, $\widehat{H}$, can be introduced:

$$\widehat{H} = \widehat{\mathcal{E}} - 4 \sum_{m=1}^{+\infty} \left| \widehat{C}_m \right|^2. \tag{40}$$

The second term of the right-hand side of equation (40) has an interesting physical meaning, as it represents the (normalized) work, $\widehat{W}$, necessary to constrain the extended vortex to its initial circular shape:

$$\widehat{W}\left(t\right) = \frac{1}{\varphi^* Q/2} \times \left[e n_0 \int_0^{2\pi} \mathrm{d}\theta \int_{r_0}^{r_0 + \varepsilon(\theta)} \left(r_0 - r\right) \widehat{\mathbf{e}}_r \cdot \nabla \mathbf{\Phi}(r, \theta, t) r \mathrm{d}r \right]. \tag{41}$$

In fact, neglecting higher-order terms (C^3 and γC^2) and integrating with respect to r, one obtains

$$\widehat{W}\left(t\right) = -\frac{1}{\pi} \int_0^{2\pi} \widehat{\varepsilon}^2\left(\theta, t\right) \mathrm{d}\theta = -4 \sum_{m=1}^{+\infty} \left| \widehat{C}_m \right|^2. \tag{42}$$

In other terms, $\widehat{W}$ can be regarded as the energy difference between the real charge distribution and its approximation (Eq. (12)), in which density waves on the border of a circular vortex are considered.

The constant of motion $\widehat{H}$ defined in equation (40) can be regarded as the Hamiltonian of the system: in fact, by writing $\widehat{C}_m = \rho_m \exp(-\mathrm{i}m\xi_m)$ and by considering the following Hamiltonian coordinates and conjugate momenta

$$q = -\sqrt{\gamma}\theta_v, \qquad p = \sqrt{\gamma} r_v^2$$
$$q_m = -\xi_m, \qquad p_m = \frac{4}{m^2} \left| \widehat{C}_m \right|^2. \tag{43}$$

Equations (22) can be deduced starting from the Hamilton's equations for the Hamiltonian $H(q, p, \{q_m\}, \{p_m\})$, as done by O'Neil *et al.* [6].

4 Analysis of vortex interaction

4.1 Resonance condition

If the interaction between the two vortices is weak, the surface waves on the finite vortex have little influence on the motion of the point vortex. In this case a simplified model can be considered, in which $\widehat{r}_v$ and $\widehat{\Omega} = \mathrm{d}\theta_v/\mathrm{d}t$ are constant:

$$\widehat{r}_v = \widehat{r}_v(0) = \mathrm{Const}$$

$$\widehat{\Omega} = \left.\frac{\mathrm{d}\theta_v}{\mathrm{d}\widehat{t}}\right|_{\widehat{t}=0} = \frac{\widehat{r}_0^2}{\widehat{r}_v^2} + \gamma\frac{\widehat{r}_0^2}{1-\widehat{r}_v^2} = \mathrm{Const}. \qquad (44)$$

As a consequence of this hypothesis, the system of equations for the contour coefficients $\left\{\widehat{C}_m\right\}$ assume the simplified form of a set of decoupled equations for each mode:

$$\frac{\mathrm{d}\widehat{C}_m}{\mathrm{d}\widehat{t}} = -\mathrm{i}mA_m\widehat{C}_m - \mathrm{i}m\frac{\gamma}{2}\widehat{G}_m(\widehat{r}_v \to \widehat{r}_0)\mathrm{e}^{-\mathrm{i}m\widehat{\Omega}\widehat{t}} \qquad (45)$$

being

$$A_m = 1 + \frac{\widehat{G}_m(\widehat{r}_0 \to \widehat{r}_0)}{\widehat{r}_0}. \qquad (46)$$

Equation (45) shows that a resonant condition is reached when $A_m = \widehat{\Omega}$. Such condition can be written explicitly as:

$$|m| + \widehat{r}_0^{2|m|} - 1 = |m|\,\widehat{r}_0^2\left[\frac{1}{\widehat{r}_v^2} + \frac{\gamma}{1-\widehat{r}_v^2}\right]. \qquad (47)$$

Equation (47) can be solved with respect to $\widehat{r}_v$; its solution, $\widehat{r}_m(\widehat{r}_0, \gamma)$, represents the resonant radius for the point vortex interacting with the mth surface mode of the finite vortex. Far from any resonance, equation (45) describes accurately the behaviour of the dynamics of the system, as shown in Figure 3, in which the time evolution of the amplitude $m = 3$ mode, as obtained by solving equation (45), is compared with the reference solution provided by the CD code. In fact, in this case each mode simply oscillates with a bounded amplitude.

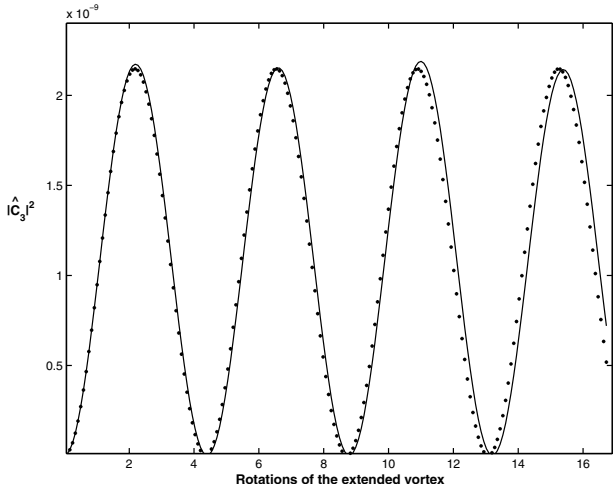

Fig. 3. Time evolution of the amplitude of the non-resonant $m = 3$ mode ($\widehat{r}_0 = 0.5$, $\widehat{r}_{v,0} = 0.648$, $\gamma = 5\times10^{-5}$), as predicted by equation (45) (dotted line) and by the CD code (full line).

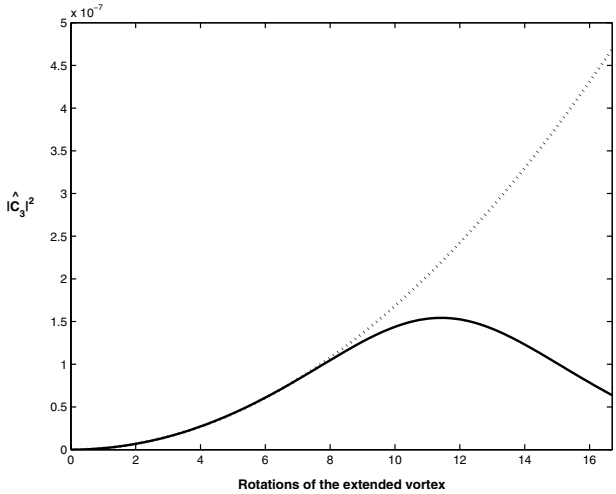

Fig. 4. Time evolution of the amplitude of the resonant $m = 3$ mode ($\widehat{r}_0 = 0.5$, $\widehat{r}_{v,0} = 0.610$, $\gamma = 5 \times 10^{-5}$), as predicted by equation (45) (dotted line) and calculated with the CD code (full line).

4.2 Trapped orbits for the point vortex

When the system is close to the resonant condition (Eq. (47)), in an early stage of the evolution the growth rate of the mth mode is far more relevant than the growth of all the others. In fact, if $A_m = \widehat{\Omega}$, the amplitude of the mth mode should grow linearly according to equation (45); however, being $\widehat{L}$ constant (Eq. (31)), a change of $|\widehat{C}_m|^2$ induces a corresponding variation in $\widehat{r}_v^2$ and the hypothesis of constant $\widehat{r}_v$ is no longer verified. A typical situation is shown in Figure 4, presenting the time evolution of the amplitude of a resonant mode obtained by solving equation (45), compared with the reference solution provided by the CD code.

To study the long-term evolution of the system when $\widehat{r}_v(0) = \widehat{r}_{v,0} \simeq \widehat{r}_m$, a different approach must be used. More precisely, starting from equations (22), a simplified analysis of the evolution can be considered, in which only the mth contour mode is present (*i.e.* setting $\widehat{C}_k(t) = 0$ for $k \neq \pm m$). By doing so, the two constants of motion, $\widehat{L}$ and $\widehat{H}$, can be used in order to express $\widehat{C}_m$ and $\widehat{C}_{-m}$ as functions of $\widehat{r}_v$, as

$$\widehat{C}_{\pm m} = \frac{1}{2}\left[\frac{\sigma_m(\widehat{r}_v)}{\beta_m(\widehat{r}_v)} \pm \sqrt{\frac{\sigma_m^2(\widehat{r}_v)}{\beta_m^2(\widehat{r}_v)} - \alpha(\widehat{r}_v)}\right]\mathrm{e}^{\mp\mathrm{i}m\theta_v} \qquad (48)$$

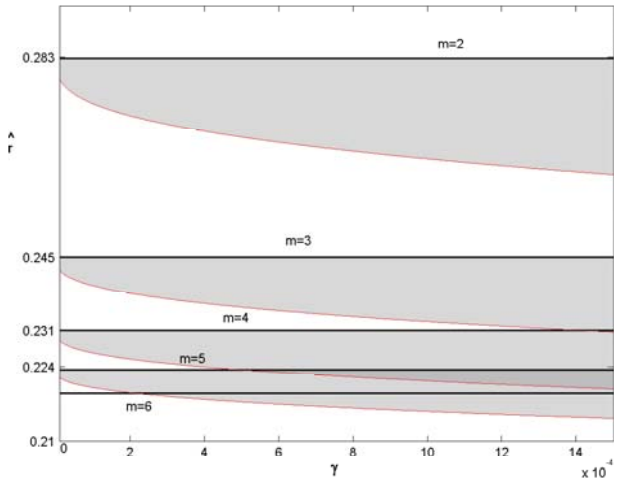

Fig. 5. Behaviour of the resonant radii, along with their respective oscillation layers (calculated by supposing $\widehat{r}_{v,0} = \widehat{r}_m$), as function of γ, for $\widehat{r}_0 = 0.2$.

being

$$\alpha\left(\widehat{r}_v\right) = \gamma(\widehat{r}_{v,0}^2 - \widehat{r}_v^2), \qquad \beta_m\left(\widehat{r}_v\right) = \frac{2\widehat{r}_0^{m+1}}{m}\gamma\left(\widehat{r}_v^{-m} - \widehat{r}_v^m\right)$$

$$\sigma_m\left(\widehat{r}_v\right) = 2\gamma\widehat{r}_0^2 \log\left(\frac{\widehat{r}_v}{\widehat{r}_{v,0}}\right) - \gamma^2\widehat{r}_0^2 \log\left(\frac{1-\widehat{r}_v^2}{1-\widehat{r}_{v,0}^2}\right) - \left(\frac{1-\widehat{r}_0^{2m}}{m} - 1\right)\alpha\left(\widehat{r}_v\right). \tag{49}$$

By inserting equation (48) into the second equation (22), one obtains a self-consistent equation for the evolution of $\widehat{r}_v$:

$$\frac{\mathrm{d}\widehat{r}_v(t)}{\mathrm{d}t} = \pm\frac{m\sqrt{f_m\left(\widehat{r}_v\right)}}{2\gamma\widehat{r}_v} \tag{50}$$

where

$$f_m\left(\widehat{r}_v\right) = \alpha\left(\widehat{r}_v\right)\beta_m^2\left(\widehat{r}_v\right) - \sigma_m^2\left(\widehat{r}_v\right). \tag{51}$$

Therefore, $\widehat{r}_v$ is forced to bounce between two zeros of $f_m\left(\widehat{r}_v\right)$, $\widehat{r}_{v,0}$ and $\widehat{r}_{v,1}$. Considering that the mean square radius of the distribution must be constant and recalling that the initial shape of the finite-size vortex is circular (*i.e.* the shape with fixed area having minimum mean square radius), one can conclude that $\widehat{r}_{v,1} < \widehat{r}_{v,0}$. Thus, the resulting dynamics of the point vortex is oscillating and the vortex remains within an annular layer of width $\Delta\widehat{r}_v = \widehat{r}_{v,0} - \widehat{r}_{v,1}$: according to these results, no merger occurs. However, if the width $\Delta\widehat{r}_v$ of the layer is large enough so that $\Delta\widehat{r}_v \sim \widehat{r}_m - \widehat{r}_{m+1}$, (being $\widehat{r}_{m+1}$ the resonant radial value for the adjacent mode $m+1$), other contour modes are excited and this leads eventually to the merger of the two vortices. Hence, a sufficient condition for the merger not to occur is $\Delta\widehat{r}_v \ll \widehat{r}_m - \widehat{r}_{m+1}$. In Figures 5, 6 and 7 the behaviour of $\widehat{r}_m$ for $m = 2, 3, 4, 5, 6$ are presented as functions of γ, for $\widehat{r}_0 = 0.2$, $\widehat{r}_0 = 0.5$ and $\widehat{r}_0 = 0.8$, together with their oscillation layers (shown as shaded areas), by supposing $\widehat{r}_{v,0} = \widehat{r}_m$.

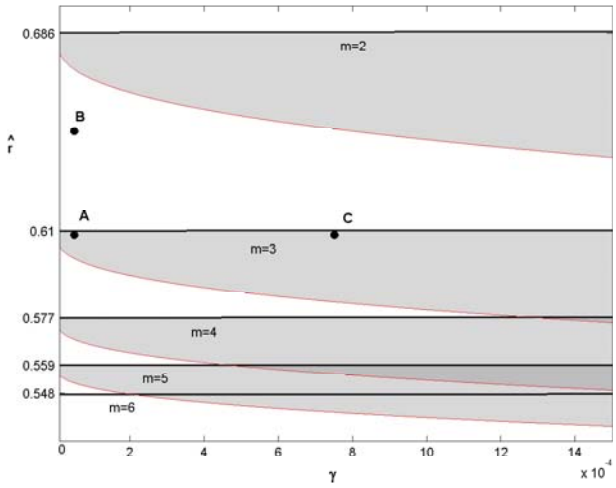

Fig. 6. Same as in Figure 5, for $\widehat{r}_0 = 0.5$.

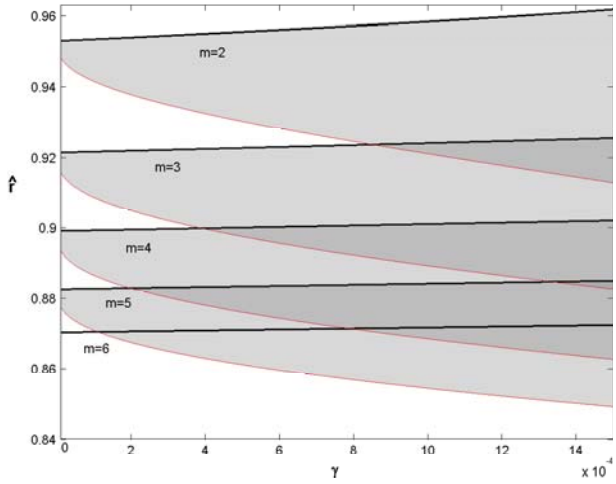

Fig. 7. Same as in Figure 5, for $\widehat{r}_0 = 0.8$.

5 Comparison with reference results

In the following, a set of results is presented, in order to prove the effectiveness of the theory using reference calculations obtained by means of a CD code [9] (all the results have been obtained by using nondimensional units, in which $R = 1$, $B_0 = 1$, $\varepsilon_0 = 1$). Referring to the previous section, three different configurations have been considered: (A) a stable configuration with initial resonant condition (according to equation (47)), (B) a stable non-resonant configuration and (C) an unstable configuration. The three configurations are indicated in Figure 6.

Figures 8 (case A), 3 and 9 (case B) show that the agreement between the results is excellent when the merging process does not occur. In fact, if the interaction between the two vortices is weak, waves of small amplitude are induced on the contour of the extended vortex and the radial coordinate of the point vortex is nearly constant in time; in this case, a first-order approximation of the problem produces accurate results. Figure 10 shows that variations of the radial coordinate of the point vortex are large in the unstable configuration (C): in this

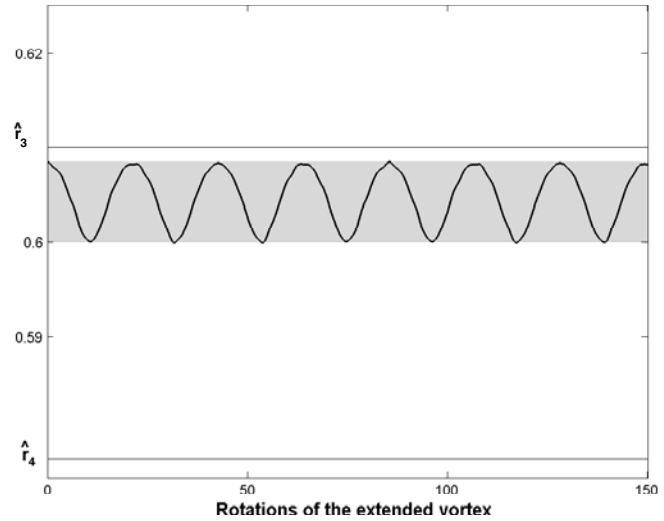

Fig. 8. Time evolution of $\widehat{r}_v$ in a stable resonant configuration (case A of Fig. 6). In this case, the curves obtained with the complete model (Eq. (22)), the simplified model (Eq. (50)), and the CD code are practically indistinguishable.

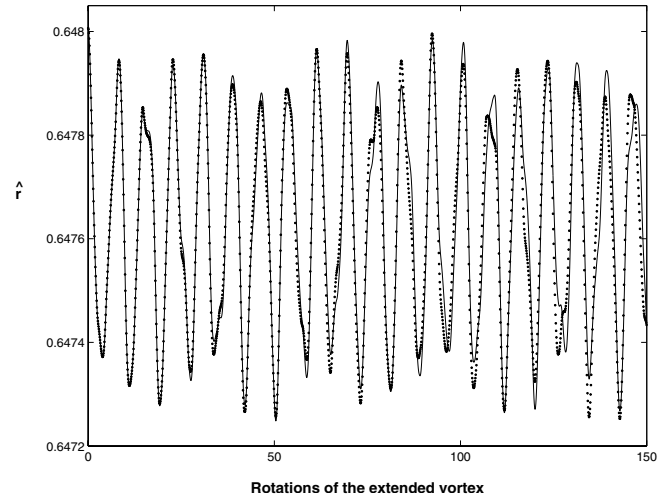

Fig. 9. Comparison between the time evolutions of $\widehat{r}_v$ in a non-resonant stable configuration (case B of Fig. 6), as obtained with the linear model (dotted line) and with the CD code (full line).

case, as the point vortex spirals towards the center of the trap, waves of increasing amplitude are produced on the contour of the finite vortex. A first-order analysis allows to describe the system only in the early stage of the merging process, until non-linear effects become relevant. Eventually, the extended vortex wraps around the point vortex, leading to the merger. This part of the process cannot be described within the present model, as at this stage the contour of the extended vortex cannot be even represented by means of a single-value function $r_c(\theta)$. A very accurate analysis of the merger has been carried out by using the CD code. In Figures 11 and 12 the complexity of the small-scale filamentation process is shown.

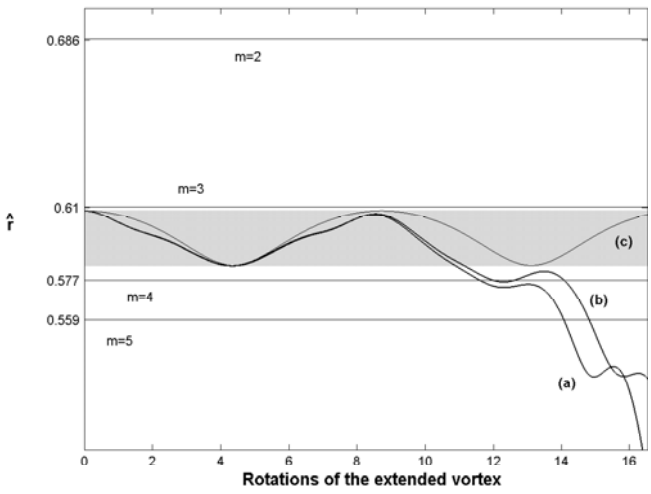

Fig. 10. Time evolution of $\widehat{r}_v$ for an unstable resonant configuration (case C of Fig. 6), as predicted by the full linear model (a), by the CD code (b) and by solving equation (50) (c).

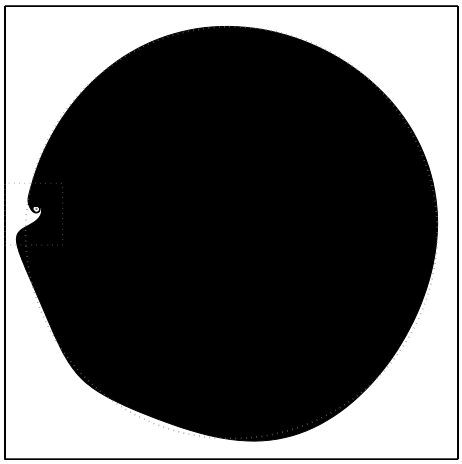

Fig. 11. Merging process between two weakly-interacting vortices: distribution after 17.5 rotations of the extended vortex (case C of Fig. 6).

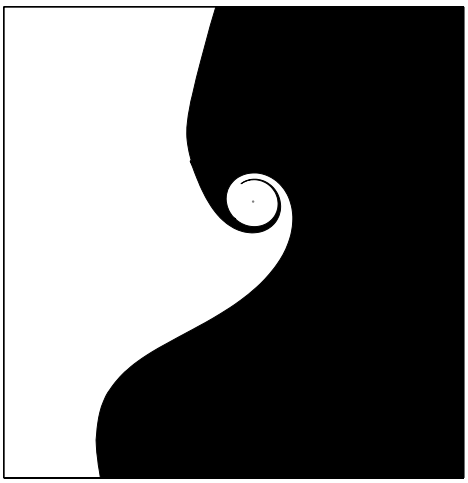

Fig. 12. Enlargement of the rectangular region marked by a dotted line in Figure 11, showing wrapping and filamentation process.

The authors wish to thank Gian Luca Delzanno for many discussions and suggestions.

References

1. N.J. Zabusky, M.H. Hughes, K.V. Roberts, J. Comput. Phys. **30**, 96 (1979)
2. K.S. Fine, C.F. Driscoll, J.H. Malmberg, T.B. Mitchell, Phys. Rev. Lett. **67**, 588 (1991)
3. T.B. Mitchell, C.F. Driscoll, K.S. Fine, Phys. Rev. Lett. **71**, 1371 (1993)
4. T.B. Mitchell, C.F. Driscoll, Phys. Fluids **8**, 1828 (1996)
5. K.S. Fine, C.F. Driscoll, J.H. Malmberg, T.B. Mitchell, Phys. Rev. Lett. **67**, 588 (1991)
6. I.M. Lansky, T.M. O'Neil, D.A. Schecter, Phys. Rev. Lett. **79**, 1479 (1997)
7. R.C. Davidson, *An introduction to the Physics of Nonneutral plasmas* (Addison-Wesley, Redwood City, 1990)
8. M. Amoretti, D. Durkin, J. Fajans, R. Pozzoli, M. Romé, Phys. Plasmas **8**, 3865 (2001)
9. G.G.M. Coppa, F. Peano, F. Peinetti, J. Comput. Phys. **182**, 392 (2002)